Solid State Ionics 192 (2011) 241–244

Contents lists available at ScienceDirect

Solid State Ionics

journal homepage: www.elsevier.com/locate/ssi

Effects of Ga substitution on the high temperature properties of the n = 3 Ruddlesden Popper system $LaSr_3Fe_{1.5-x/2}Co_{1.5-x/2}Ga_xO_{10-\delta}$ $(0 \le x \le 0.8)$

F. Prado [a,b,*], J.-H. Kim [a], A. Manthiram [a]

[a] Electrochemical Energy Laboratory and Materials Science and Engineering Program, University of Texas at Austin, Austin, Texas 78712, USA
[b] Departamento de Física, Universidad Nacional del Sur, 8000 Bahía Blanca, Argentina

ARTICLE INFO

Article history:
Received 30 August 2009
Received in revised form 20 May 2010
Accepted 28 May 2010
Available online 26 June 2010

Keywords:
Mixed conductors
Ruddlesden Popper phases
Crystal structure
Thermal expansion
Solid oxide fuel cells

ABSTRACT

The effects of the Ga incorporation on the crystal chemistry and high temperature properties of the n = 3 Ruddlesden Popper system $LaSr_3Fe_{1.5-x/2}Co_{1.5-x/2}Ga_xO_{10-\delta}$ $(0 \le x \le 0.8)$ have been investigated. As the Ga content increases the symmetry of the unit cell varies from tetragonal for the samples with x = 0 and 0.3 to orthorhombic for the x = 0.8 sample. Due to the fixed Ga^{+3} oxidation state, the substitution of Ga for Fe and Co increases the oxygen vacancy concentration in the samples at room temperature while it decreases the variation of the oxygen content with temperature. The total expansion coefficient of the $LaSr_3Fe_{1.5-x/2}Co_{1.5-x/2}Ga_xO_{10-\delta}$ specimen in the temperature range $80 \le T \le 900$ °C decreases with increasing Ga content due to the suppression of the chemical expansion at high temperature. Similarly, the electrical conductivity also decreases as the Ga content increases. The electrochemical performances of the $LaSr_3Fe_{1.5-x/2}Co_{1.5-x/2}Ga_xO_{10-\delta}$ samples as cathode materials in SOFC have been tested with electrolyte-supported single cells using $La_{0.8}Sr_{0.2}Ga_{0.8}Mg_{0.2}O_{2.8}$ (LSGM) as an electrolyte. Although the maximum power density of the cells decreases with increasing Ga content, the $LaSr_3Fe_{1.5-x/2}Co_{1.5-x/2}Ga_xO_{10-\delta}$ cathode provides an important advantage of decrease in total expansion with increasing Ga content.

1. Introduction

The mixed oxide ion and electronic conducting properties of the Ruddlesden Popper (R-P) series of oxides $A_{n+1}B_nO_{3n+1}$ with n = 1, 2 and 3 have been explored in the recent years to evaluate their use at high temperatures as cathodes in SOFC and oxygen separation membranes [1–5]. The crystal structure of the R-P phases consists of *n* ABO_3 perovskite layers alternating with AO rock salt layers along the c-axis [6]. Previous work has focused on the synthesis and oxygen permeation properties of the n = 3 R-P solid solution $LaSr_3Fe_{3-x}Co_xO_{10-\delta}$ with $0 \le x \le 1.5$ [4,5]. These studies have shown that the x = 1.5 compound exhibits good structural stability combined with adequate values of oxide ion and electronic conductivity [4] for electrochemical applications. In an attempt to increase the oxygen vacancy concentration and thereby to improve the oxide-ion conductivity, Ga has been incorporated in the B site and the solid solution $LaSr_3GaFe_{2-x}Co_xO_{10-\delta}$ has been investigated [7]. However, the presence of 1/3 of Ga in the B site has induced a structural transformation from tetragonal to orthorhombic [7,8] affecting the mixed conducting properties. More recently, Lee and Manthiram [9] have found that $LaSr_3Fe_{1.5}Co_{1.5}O_{10-\delta}$ exhibits cathode performance in SOFC comparable to the perovskite phase $La_{0.6}Sr_{0.4}CoO_{3-\delta}$. Although the total expansion coefficient $\alpha = 20.5 \times 10^{-6}\,K^{-1}$ was lower than that of the perovskite phase, it was still higher than the values exhibited by the GDC or LSGM electrolytes ($\sim 10–12 \times 10^{-6}\,K^{-1}$). With an aim to develop a mixed conductor with lower total lattice expansion, we present here the incorporation of Ga into the B sites of the composition $LaSr_3Fe_{1.5}Co_{1.5}O_{10-\delta}$, keeping the Fe:Co ratio constant at 1, and discuss the effects of Ga substitution on the crystal structure, lattice expansion, electrical conductivity, and electrochemical performance.

2. Experimental

The $LaSr_3Fe_{1.5-x/2}Co_{1.5-x/2}Ga_xO_{10-\delta}$ samples were prepared by solid state reactions of stoichiometric amounts of La_2O_3, $SrCO_3$, Fe_2O_3, Co_3O_4, and Ga_2O_3. The powders were heat treated first at 900 °C and then pressed and sintered at temperatures ranging between 1300 and 1350 °C. Both heat treatments were carried out in air for 24 h. In addition, the powders were ball milled in ethanol for 1 day before each heat treatment. The resulting materials were then heat treated at 600 °C for 6 h in air followed by slow cooling to room temperature at a rate of 1 °C/min to maximize the oxygen content. The $La_{0.8}Sr_{0.2}Ga_{0.8}Mg_{0.2}O_{2.8}$ (LSGM) electrolyte disks, interlayer materials $Ce_{0.9}Gd_{0.1}O_{1.95}$ (GDC) and $La_{0.4}Ce_{0.6}O_{1.8}$ (LDC), and Ni/GDC anode composite (Ni:GDC = 70:30 vol.%) were prepared following the procedures described elsewhere [10]. X-ray diffraction (XRD) data were collected using Cu Kα radiation and a graphite monochromator from 2θ = 10 to 100º with a counting time of 10 s per 0.02º. The crystal

* Corresponding author. Departamento de Física, Universidad Nacional del Sur, 8000 Bahía Blanca, Argentina. Tel.: +54 291 4595168; fax: +54 291 4595142.
E-mail address: fernando.prado@uns.edu.ar (F. Prado).

0167-2738/$ – see front matter © 2010 Elsevier B.V. All rights reserved.
doi:10.1016/j.ssi.2010.05.056

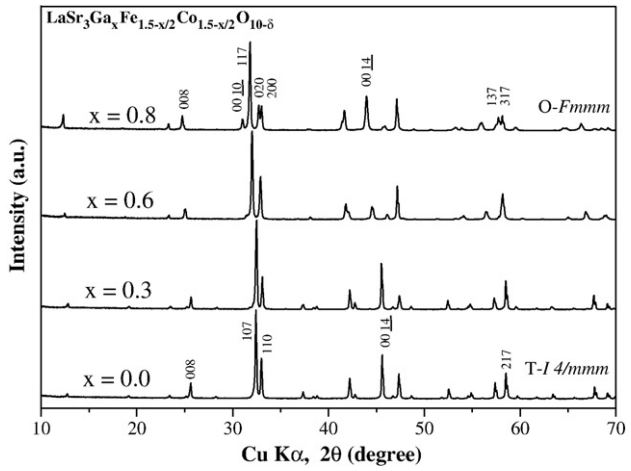

Fig. 1. X-ray diffraction patterns of the $LaSr_3Fe_{1.5-x/2}Co_{1.5-x/2}Ga_xO_{10-\delta}$ samples with x = 0, 0.3, 0.6, and 0.8. The reflections are indexed to follow the symmetry transformation of the unit cell.

structures of the samples were analyzed by the Rietveld method using the FullProf Program [11]. The average oxidation state of (Fe/Co) and the room temperature oxygen content of the samples were determined by iodometric titration [12]. The TEC values were measured in air in the temperature range 80–900 °C with a heating/cooling rate of 5 °C/min using a Perkin-Elmer Series 7 thermal analysis system. Electrical conductivity measurements were carried out in air in the temperature range $20 \le T \le 900$ °C using a four-probe dc technique on disc samples with the Van der Pauw configuration. The single cells were constructed using 0.5 mm thick disks of LSGM as electrolyte, $NiO–Ce_{0.9}Gd_{0.1}O_{1.95}$ as anode, and $LaSr_3Fe_{1.5-x/2}Co_{1.5-x/2}Ga_xO_{10-\delta}$ as cathode. To prevent the reaction of the electrodes with the electrolyte, GDC and LDC were used as buffer layers, respectively, onto the cathode and anode sides of LSGM. Electrodes and buffer layers were deposited on an area of 5 × 5 mm by screen printing. The slurry preparation and deposition and heat treatment sequence are available elsewhere [10]. Pt mesh attached to Pt wires was used as current collector. The thickness, microstructure, and LSGM-electrodes interfaces of the single cells were analyzed with a JEOL-5610 scanning electron microscope (SEM). The electrochemical performances were evaluated in the temperature range $600 \le T \le 800$ °C. During the single-cell performance test, humidified H_2 (3% H_2O at 25 °C) was supplied at the anode as fuel and air at the cathode as oxidant at a rate of 100 cm^3/min.

Table 1
Oxygen content, average oxidation state, and crystal symmetry of $LaSr_3Fe_{1.5-x/2}Co_{1.5-x/2}Ga_xO_{10-\delta}$ at 20 °C.

Ga content, x	Oxygen content	Oxidation state of (Fe/Co)	Crystal symmetry
0	10.04 ± 0.03	3.7	*I4/mmm*
0.3	9.9 ± 0.04	3.67	*I4/mmm*
0.6	9.53 ± 0.02	3.44	*Fmmm*
0.8	9.18 ± 0.03	3.16	*Fmmm*
1.0 [a]	9.11 ± 0.03	3.11	*Fmmm*

[a] Data from Ref. [7].

3. Results and discussion

The XRD patterns of the $LaSr_3Fe_{1.5-x/2}Co_{1.5-x/2}Ga_xO_{10-\delta}$ samples with x = 0, 0.3, 0.6 and 0.8 are shown in Fig. 1. The analysis of the XRD data using the Rietveld method indicates that the samples are single phase. The symmetry of the crystal structure changes from tetragonal (S.G. *I* 4/*mmm*) for samples with x = 0 and 0.3 to orthorhombic (S.G. *Fmmm*) for samples with $x \ge 0.6$ [2]. Different models have been tried to refine the x = 0.6 sample crystal structure. The best refinement was obtained with the orthorhombic symmetry. After the transformation, the tetragonal cell of dimensions $a_T \times a_T \times c_T$ is rotated 45º to give the orthorhombic dimensions $a_O \approx \sqrt{2}a_T \times b_O \approx \sqrt{2}a_T \times c_O \approx c_T$. The variations of the lattice parameters with the Ga content are shown in Fig. 2. Besides the splitting of the lattice parameter *a*, a clear increase in the lattice parameter *c* is observed in the orthorhombic phase. This behavior is associated with a decrease in the oxygen content and the average oxidation state for (Fe/Co) as the Ga content varies from 0 to 1.0 (Table 1).

Fig. 3 shows the total linear expansion ($\Delta L/L_0$) vs. T curves for $LaSr_3Fe_{1.5-x/2}Co_{1.5-x/2}Ga_xO_{10-\delta}$. For the samples with $x \le 0.6$, the total linear expansion contains both the thermal and chemical contributions. The latter is distinguished by an increase in slope at $T \ge 500$ °C caused by the removal of oxygen atoms from the crystal lattice. The incorporation of an element with fixed oxidation state like Ga^{+3} reduces the variations in the oxygen content causing a systematic decrease in the chemical contribution and thereby in the total expansion of $LaSr_3Fe_{1.5-x/2}Co_{1.5-x/2}Ga_xO_{10-\delta}$. The variations of the total expansion coefficient $\alpha = \frac{\Delta L}{\Delta T \times L_0}$ with Ga content for the temperature ranges $80 \le T \le 900$ °C; $80 \le T \le 700$ °C and $80 \le T \le 500$ °C are shown in the inset of Fig. 3. The reduction of α is more significant for the x = 0.8 sample with orthorhombic symmetry, reaching a value $\alpha = 12.9 \times 10^{-6}$ (K^{-1}) almost constant with temperature.

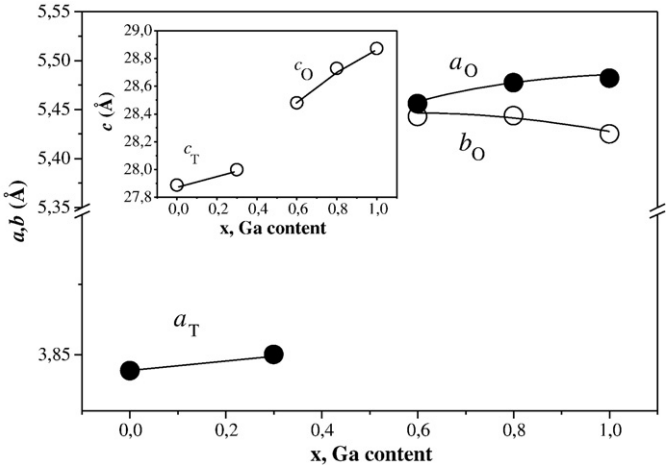

Fig. 2. Variations of the lattice parameters *a* and *b* of the crystal structure of $LaSr_3Fe_{1.5-x/2}Co_{1.5-x/2}Ga_xO_{10-\delta}$ with the Ga content x. The inset shows the variation of the lattice parameter *c* with x.

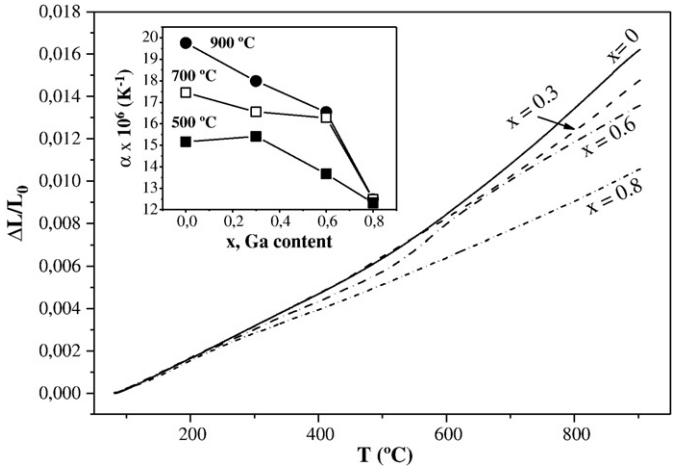

Fig. 3. $\Delta L/L_0$ vs. T curves of the $LaSr_3Fe_{1.5-x/2}Co_{1.5-x/2}Ga_xO_{10-\delta}$ samples with x = 0, 0.3, 0.6, and 0.8. The inset shows the total expansion coefficient α calculated for the temperature range ●) 80–900 °C, □) 80–700 °C, and ○) 80–500 °C.

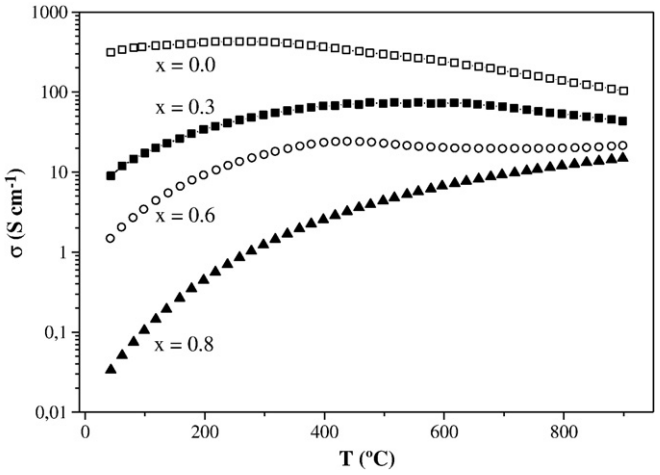

Fig. 4. Variations of the total conductivity with temperature for $LaSr_3Fe_{1.5-x/2}Co_{1.5-x/2}Ga_xO_{10-\delta}$ in air for $0 \le x \le 0.8$.

Fig. 4 shows the variations of the electrical conductivity (σ) with temperature in the range $20 \le T \le 900$ °C. The replacement of Fe and Co by Ga affects the O–(Fe/Co)–O extended interaction in different ways: a) the O–Fe/Co–O covalency decreases as the Fe/Co–O bond length enlarge with the addition of Ga^{+3}, and b) the presence of Ga^{+3} itself with pseudo-inert gas configuration along with the increasing concentration of oxygen vacancies at a given temperature reduce the available electronic states leading to a larger electron localization. This effect is more significant at room temperature where a difference of approximately four orders of magnitude between the σ values of the $x = 0$ and 0.8 samples is observed. Above room temperature, the electrical conductivity was found to be thermally activated for all the samples. In the high temperature region ($T \ge 400$–500 °C), samples with low Ga content ($x = 0$ and 0.3) begin to lose oxygen, which causes a decrease in the electrical conductivity with temperature. On the other hand, the $x = 0.8$ sample exhibits a thermally activated behavior for the whole temperature range. As a consequence, the difference in the σ values at T ~ 800–900 °C is approximately one order of magnitude.

Chemical reactivity tests were carried out by annealing the cathode materials $LaSr_3Fe_{1.5-x/2}Co_{1.5-x/2}Ga_xO_{10-\delta}$ mixed with LSGM and GDC at 1000 and 1100 °C in air for three hours. The analysis of the powder XRD data of the final products indicates that while $LaSr_3Fe_{1.5-x/2}Co_{1.5-x/2}Ga_xO_{10-\delta}$ reacts with LSGM at 1100 °C, no evidence of reaction with GDC was detected. Based on this result, GDC was used as an interlayer between the cathode and LSGM. Similarly, to avoid the chemical reaction between Ni and LSGM at the firing temperature of the anode material ($T = 1300$ °C), the cells were prepared using LDC as an interlayer between the GDC + Ni cermet anode and LSGM [9,10]. SEM micrographs of the single-cell cross sections including cathode, GDC interlayer, and the electrolyte are shown in Fig. 5 for the cathode materials with $x = 0$, 0.3, and 0.6 after testing the cells in the temperature range $600 \le T \le 800$ °C. The thickness of the layers obtained by screen printing at the cathode side was around 25–30 μm for the cathode and 3–4 μm for the GDC interlayer material. In Fig. 5c, the electron backscattering image of the cell cross section clearly reveals the uniformity of the interlayer material. Finally, the microstructure of the cathode materials appears to be quite similar for all the samples suggesting that the variations of the electrochemical performance are due to the variations in the composition of the cathodes and not due to changes in the microstructure.

From the electrochemical tests of the $LaSr_3Fe_{1.5-x/2}Co_{1.5-x/2}Ga_xO_{10-\delta}$/GDC/LSGM/LDC/Ni–GDC single cells, we have obtained the variations of the cell voltage (V) and power density (P) as a function of current density (I) for various cathodes materials. Measurements were performed by heating the cell at 800 °C and then lowering the temperature in steps of 50 °C until reaching 600 °C. Typical V–I and P–I curves obtained for the $x = 0$ sample are displayed in the inset of Fig. 6. The variations of the maximum power density (P_{max}) delivered by the cells as a function of the temperature for the $x = 0$, 0.3, and 0.6 cathodes are shown in Fig. 6. The best performance was obtained for the Ga-free $LaSr_3Fe_{1.5}Co_{1.5}O_{10-\delta}$ cathode with a P_{max} value of 0.42 W/cm^2 at 800 °C. The incorporation of Ga in the cathode reduces the performance of the

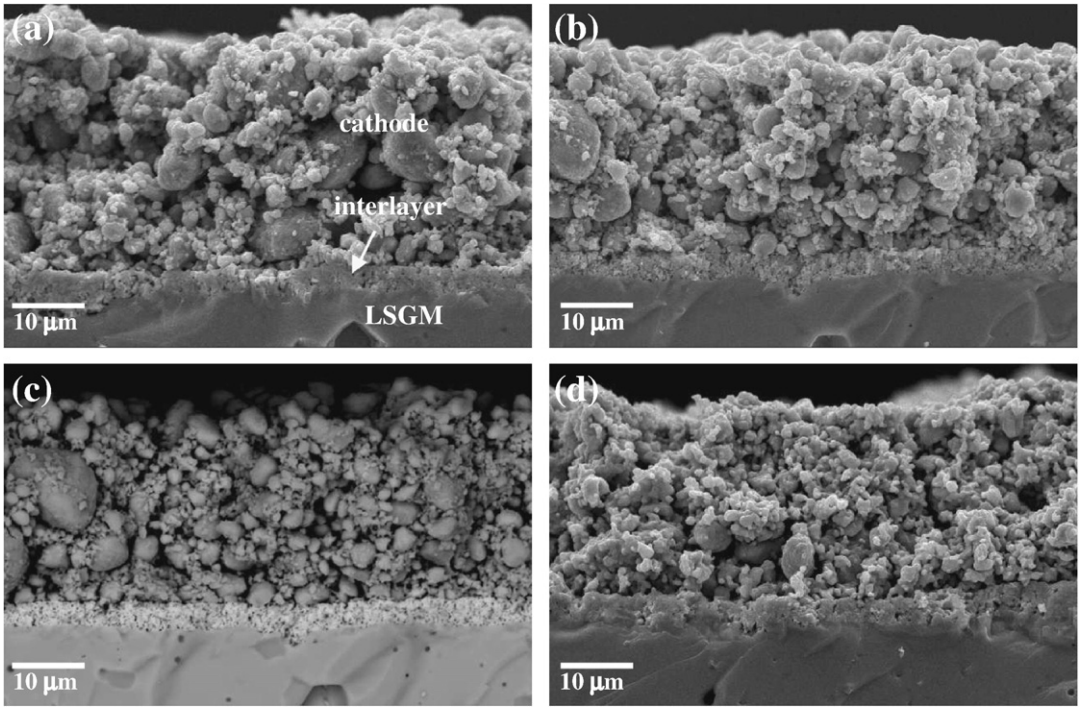

Fig. 5. SEM micrographs of the $LaSr_3Fe_{1.5-x/2}Co_{1.5-x/2}Ga_xO_{10-\delta}$ cathodes with GDC interlayer on the LSGM electrolyte: (a) $x = 0$, (b) $x = 0.3$, (c) electron backscattering image of the $x = 0.3$ sample, and (d) $x = 0.6$.

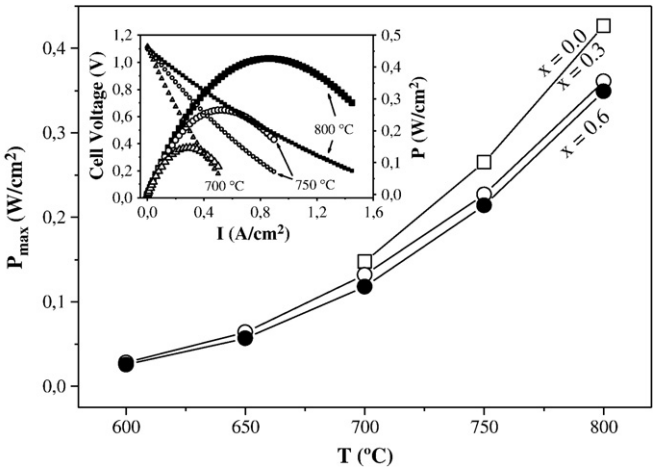

Fig. 6. Maximum power density of $LaSr_3Fe_{1.5-x/2}Co_{1.5-x/2}Ga_xO_{10-\delta}$/GDC/LSGM/LDC/Ni–GDC single cells as a function of temperature. The inset shows the variations of the cell voltage and the power density with current density for the $x=0$ cathode at 800, 750, and 700 °C.

cell, leading to a maximum power of 0.35 W/cm^2 at 800 °C for the $x=0.6$ cathode.

4. Conclusions

The $n=3$ member of the R-P series of phases $LaSr_3Fe_{1.5-x/2}Co_{1.5-x/2}Ga_xO_{10-\delta}$ with $0\leq x\leq 0.8$ have been synthesized and characterized as cathodes for SOFC. The incorporation of Ga into the crystal lattice of $LaSr_3Fe_{1.5}Co_{1.5}O_{10-\delta}$ causes a (i) transformation of the unit cell symmetry from tetragonal to orthorhombic, (ii) suppression of the chemical contribution to the total thermal expansion, and (iii) reduction of the electrical conductivity. The electrochemical performances of these R-P phases as cathode material have been tested with electrolyte-supported single cells using LSGM as the electrolyte. Although the presence of Ga^{+3} reduces the maximum power delivered by the cell, the lowering of the total expansion coefficient may be helpful to realize better compatibility with the electrolyte.

Acknowledgement

Financial support by the Welch Foundation grant F-1254 in the United States of America and CONICET and ANPCyT through PICT 2006-00829 and 2007-02288 in Argentina is gratefully acknowledged.

References

[1] V.V. Vashook, N.E. Trofimenko, H. Ullmann, L.V. Makhnach, Solid State Ionics 131 (2000) 329.
[2] G. Amow, I.J. Davison, S.J. Skinner, Solid State Ionics 177 (2006) (2010) 1205.
[3] F. Prado, T. Armstrong, A. Caneiro, A. Manthiram, J. Electrochem. Soc. 148 (2001) J7.
[4] T. Armstrong, F. Prado, A. Manthiram, Solid State Ionics 140 (2001) 89.
[5] A. Manthiram, F. Prado, T. Armstrong, Solid State Ionics 152–153 (2002) 647.
[6] S.N. Ruddlesden, P. Popper, Acta Cryst. 11 (1958) 54.
[7] F. Prado, K. Gurunatham, A. Manthiram, J. Mater. Chem. 12 (2002) 2390.
[8] B. Shankar, H. Steinfink, J. Solid State Chem. 122 (1996) 390.
[9] K.T. Lee, A. Manthiram, Chem. Mater. 18 (2006) 1621.
[10] J.-H. Kim, F. Prado, A. Manthiram, J. Electrochem. Soc. 155 (2008) B1023.
[11] J. Rodríguez-Carvajal, Fullprof: a program for Rietveld Refinement and Profile Matching Analysis of Complex Powder Diffraction Patterns, Laboratoire Léon Brillouin (CEA-CNRS).
[12] A. Manthiram, J.S. Swinnea, Z.T. Sui, H. Steinfink, J.B. Goodenough, J. Am. Chem. Soc. 109 (1987) 6667.